Published OnlineFirst February 15, 2011; DOI: 10.1158/1078-0432.CCR-10-1694

Cancer Therapy: Preclinical

Clinical Cancer Research

Antitumor Efficacy of PKI-587, a Highly Potent Dual PI3K/mTOR Kinase Inhibitor

Robert Mallon[1], Larry R. Feldberg[1], Judy Lucas[1], Inder Chaudhary[3], Christoph Dehnhardt[2], Efren Delos Santos[2], Zecheng Chen[2], Osvaldo dos Santos[2], Semiramis Ayral-Kaloustian[2], Aranapakam Venkatesan[2], and Irwin Hollander[1]

Abstract

Purpose: The aim of this study was to show preclinical efficacy and clinical development potential of PKI-587, a dual phosphoinositide 3-kinase (PI3K)/mTOR inhibitor.

Experimental Design: *In vitro* class 1 PI3K enzyme and human tumor cell growth inhibition assays and *in vivo* five tumor xenograft models were used to show efficacy.

Results: *In vitro*, PKI-587 potently inhibited class I PI3Ks (IC_{50} vs. PI3K-α = 0.4 nmol/L), PI3K-α mutants, and mTOR. PKI-587 inhibited growth of 50 diverse human tumor cell lines at IC_{50} values of less than 100 nmol/L. PKI-587 suppressed phosphorylation of PI3K/mTOR effectors (e.g., Akt), and induced apoptosis in human tumor cell lines with elevated PI3K/mTOR signaling. MDA-MB-361 [breast; $HER2^+$, *PIK3CA* mutant (E545K)] was particularly sensitive to this effect, with cleaved PARP, an apoptosis marker, induced by 30 nmol/L PKI-587 at 4 hours.

In vivo, PKI-587 inhibited tumor growth in breast (MDA-MB-361, BT474), colon (HCT116), lung (H1975), and glioma (U87MG) xenograft models. In MDA-MB-361 tumors, PKI-587 (25 mg/kg, single dose i.v.) suppressed Akt phosphorylation [at threonine(T)308 and serine(S)473] for up to 36 hours, with cleaved PARP (cPARP) evident up to 18 hours. PKI-587 at 25 mg/kg (once weekly) shrank large (~1,000 mm^3) MDA-MB-361 tumors and suppressed tumor regrowth. Tumor regression correlated with suppression of phosphorylated Akt in the MDA-MB-361 model. PKI-587 also caused regression in other tumor models, and efficacy was enhanced when given in combination with PD0325901 (MEK 1/2 inhibitor), irinotecan (topoisomerase I inhibitor), or HKI-272 (neratinib, HER2 inhibitor).

Conclusion: Significant antitumor efficacy and a favorable pharmacokinetic/safety profile justified phase 1 clinical evaluation of PKI-587. *Clin Cancer Res; 17(10); 3193–203. ©2011 AACR.*

Introduction

Class 1 phosphoinositide 3-kinases (PI3K) play a key role in the biology of human cancer. The gene encoding the PI3K-α isoform (*PIK3CA*) is amplified or mutated in a wide range of cancers (1, 2). Aberrantly elevated PI3K/Akt/mTOR pathway signaling has been implicated in poor prognosis and survival in patients with lymphatic, breast, prostate, lung, glioblastoma, melanoma, colon, and ovarian cancers (1–6). In addition, PI3K/Akt/mTOR pathway activation contributes to resistance of cancer cells to both targeted anticancer therapies and conventional cytotoxic agents (5, 6). An effective inhibitor of the PI3K/Akt/mTOR pathway could prevent cancer cell proliferation and induce programmed cell death (apoptosis; refs. 1, 2, 5). Many pharmaceutical companies now have substantial PI3K/mTOR signaling pathway inhibitor programs. Examples of advanced dual PI3K/mTOR inhibitors include: BEZ-235 (Novartis), BGT-226 (Novartis), XL765 (Exelixis), SF1126 (Semafore), and PKI-402 (Wyeth/Pfizer) (7–11). Examples of advanced inhibitors selective for class 1 PI3Ks include: GDC-0941 (Genentech), XL147 (Exelixis), BKM120 (Novartis), GSK1059615 (Glaxo), CAL101 (Calistoga), and PX-866 (Oncotheryon) (7, 8, 12–14). BEZ-235 and BGT-226 are in phase 2, whereas most other compounds are undergoing phase 1 clinical evaluation (7, 8).

The Wyeth PI3K inhibitor discovery project identified PKI-587, an exceptionally potent, selective, ATP-competitive, and reversible PI3K/mTOR inhibitor for clinical development (15). *In vivo*, PKI-587 displayed antitumor activity (i.v. route) in breast (MDA-MB-361, BT474), colon (HCT116), glioma (U87MG), and non–small cell lung cancer [(NSCLC) H1975] xenograft models. PKI-587 caused tumor regression in some models and its favorable

Authors' Affiliations: Departments of [1]Oncology, [2]Discovery Medicinal Chemistry, and [3]Drug Safety and Metabolism, Wyeth Research (now Pfizer), Pearl River, New York

Note: Supplementary data for this article are available at Clinical Cancer Research Online (http://clincancerres.aacrjournals.org/).

Corresponding Author: Robert Mallon, Wyeth Research (now Pfizer) 401 N. Middletown Rd, Pearl River, NY 10965. Phone: 973-747-5906; Fax: 973-618-9991. E-mail: mallonrg@gmail.com

doi: 10.1158/1078-0432.CCR-10-1694

Published OnlineFirst February 15, 2011; DOI: 10.1158/1078-0432.CCR-10-1694

Translational Relevance

PKI-587, a potent pan–class I phosphoinositide 3-kinase (PI3K)/mTOR inhibitor, showed single-agent efficacy in multiple preclinical tumor models. Tumor regression was observed in several models. This effect was most pronounced against MDA-MB-361 (breast), which has elevated HER2 levels and mutant PI3K-α. Preclinical data suggest utility of PKI-587 in the treatment of cancers with elevated PI3K/mTOR signaling, including those resistant to agents that target HER2 or epidermal growth factor (EGF) receptors (EGFR).

PKI-587 efficacy was enhanced when combined with a MEK1,2 kinase inhibitor (PD0325901), or irinotecan in a colon tumor model (HCT116) with mutant *K-Ras*. PKI-587 showed single-agent efficacy against a non–small cell lung cancer model (H1975) with mutant *EGFR* (L858R/T790M), and this activity was also enhanced when combined with the irreversible HER2 kinase inhibitor, HKI-272. These preclinical data suggest strategies for clinical targeting and combination uses of PKI-587.

efficacy, pharmacokinetic, and safety profile advanced it to phase 1 clinical evaluation.

Materials and Methods

Enzyme assays

Enzyme assays were done in fluorescent polarization format as previously described (11, 16, 17). PKI-587 selectivity was evaluated in the Invitrogen 236 human kinase panel, at [ATP] = K_m for each enzyme.

Cell culture, growth inhibition, and translocation assays

All cell lines, except U2OS, were from American Type Culture Collection. Mutational status (Table 1) of various oncogenes in cell lines was from the Wellcome Trust Sanger Institute site (18). PKI-587 was tested in additional human tumor cell lines by Caliper Life Sciences (Supplementary Table S1).

U2OS cells, engineered to monitor FOXO1-GFP cellular translocation, were from Thermo Scientific. Cell growth inhibition and FOXO-GFP translocation assays were done as previously described (17).

Cell lines were propagated as recommended by suppliers.

Cell lysis and Western blotting

Cells were exposed to PKI-587 for 4 hours (unless indicated otherwise in the following text). Cell lysis and lysate handling were done as previously described (11, 17). Antibodies were from Cell Signaling Technology. Inhibition of protein phosphorylation was quantified from Western blots, using the BioRad Fluor-S MultiImager with Quantity One Analysis software.

Caspase activation assay

Cellular caspase 3/7 activity was measured by the Caspase-Glo 3/7 Luminescent Assay (Promega). Cells were exposed to PKI-587 for 4 to 24 hours, and assay format and data collection were as previously described (17).

Establishment of xenograft tumors, efficacy studies, and biomarker analysis

In vivo methodology was carried out as previously described (11, 17). PKI-587 or vehicle (5% dextrose, water, pH 3.5) was administered by i.v. route in various regimens: daily or intermittent (days 1, 5, 9, etc.). *In vivo* studies were conducted under an approved Institutional Animal Care and Use Committee protocol. Significant (statistically, Student's *t* test) reduction in the tumor growth of treated groups compared with controls (vehicle) was defined as a value of $P < 0.05$.

Pharmacokinetic and pharmacodynamic (biomarker) measurements were done on tumor-bearing female nude mice administered PKI-587. Tissue samples were processed and probed with the various antibodies as described previously (11, 17).

Results

Enzyme assays

PKI-587 (Fig. 1), an ATP-competitive triazine scaffold compound (Supplementary Table S2), potently inhibited PI3K-α (IC_{50} = 0.4 nmol/L). Mutant forms of PI3K-α with elevated lipid kinase activity (19) were inhibited by PKI-587 at concentrations equivalent to the IC_{50} for wild-type PI3K-α. PI3K-β, δ, and γ isoforms were inhibited by PKI-587 at concentrations approximately 10-fold higher than that observed for PI3K-α. mTOR kinase inhibition (IC_{50} = 1 nmol/L) indicated that PKI-587 was an equipotent PI3K-α/mTOR inhibitor.

PKI-587 showed a highly selective profile when tested against 236 human protein kinases (IC_{50} > 10 μmol/L, Supplementary Table S3; Invitrogen). Only wild-type and mutant (V600E) *B-Raf*s were inhibited by PKI-587 at IC_{50} values of 10 μmol/L.

Cell growth inhibition assay

PKI-587 was a potent cell growth inhibitor with IC_{50} values of 50 nmol/L or less in 19 of 23 human tumor cell lines (Table 1). PKI-587 was also a potent cell growth inhibitor (IC_{50} < 100 nmol/L) in 37 of 43 tumor cell lines (from the NCI-60) assayed by Caliper Life Sciences (Supplementary Table S1). PKI-587 suppressed phosphorylation of downstream effectors of PI3K signaling (e.g., Akt at T308) at concentrations that closely matched growth inhibition IC_{50} values in MDA-MB-361, BT474, HCT116, H1975, U87MG, and A498. Phosphoblot data for BT474 and U87MG, as well as A498 and 786-0 with/without 10 μmol/L verapamil (see later), are shown in Supplementary Figure S1A and B.

Higher IC_{50} values against A498, 786-0, H1299, and DLD1 (IC_{50} range = 267–433 nmol/L, Table 1) were

Published OnlineFirst February 15, 2011; DOI: 10.1158/1078-0432.CCR-10-1694

Table 1. Tumor cell growth inhibition by PKI-587

Cell line	Tissue	Mutations	IC_{50}, μmol/L	σ
MDA-MB-361	Breast	*HER2*,[a]*PIK3CA*	0.001	0.0009
MDA-MB-231	Breast	*K-Ras*, *B-Raf*	0.042	0.002
MDA-MB-468	Breast	*PTEN*	0.006	0.001
T47D	Breast	*PIK3CA*	0.002	0.001
MCF7	Breast	*PIK3CA*	0.036	0.005
BT474	Breast	*HER2*,[a]*PIKC3A*	0.007	0.001
HT29	Colon	*B-Raf*	0.037	0.004
HCT116	Colon	*K-Ras*, *PIKC3A*	0.008	0.001
DLD1	Colon	*K-Ras*, *PIKC3A*	0.31	0.056
U87	Glioma	*PTEN*	0.012	0.002
H157	NSCLC	*K-Ras*, *PIKC3A*	0.013	0.002
H460	NSCLC	*K-Ras*, *PIKC3A*	0.05	0.007
A549	NSCLC	*K-Ras*	0.02	0.003
H1975	NSCLC	*EGFR*	0.014	0.005
H1650	NSCLC	*EGFR*	0.024	0.01
H2170	NSCLC	*TP53*	0.041	0.009
H1666	NSCLC	*STK11* (*LKB1*)	0.027	0.005
H1299	NSCLC	*N-Ras*	0.267	0.031
KB	Epidermoid	–	0.005	0.001
786-0	Kidney	*PTEN*, *VHL*	0.421	0.031
HTB44	Kidney	*VHL*	0.433	0.07
MIA PaCa	Pancreas	*K-Ras*	0.022	0.005
PC3	Prostate	*PTEN*	0.011	0.001

[a]HER2 amplification.

investigated. Drug efflux capacity sensitive to the L-type calcium channel and P-glycoprotein (multidrug resistance) inhibitor verapamil (20) was reported for these cell lines (21, 22). PKI-587 growth inhibition in these cells was reevaluated in the presence of 10 μmol/L verapamil, which blocks P-glycoprotein function but does not affect cell growth or viability. A498, 786-0, H1299, and DLD1 exposed to PKI-587 with 10 μmol/L verapamil had 4- to 9-fold lower growth inhibition IC_{50} values (Supplementary Table S4). Therefore, A498, 786-0, H1299, and DLD1 "resistance" to PKI-587 was related to verapamil-sensitive compound efflux and not a PI3K/Akt/mTOR signaling pathway–independent mechanism.

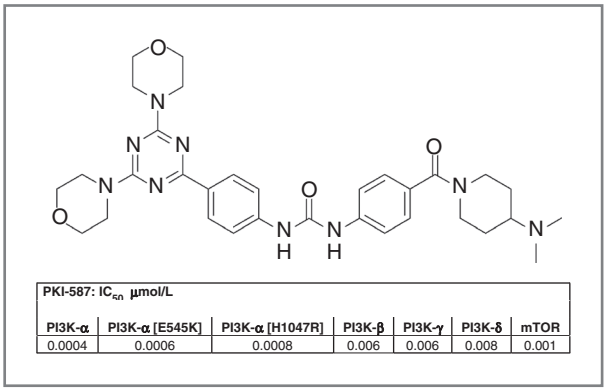

Figure 1. PKI-587 structure and IC_{50} data (μmol/L) for class I PI3Ks, the most frequently occurring mutant forms of PI3K-α (E545K, H1047R), and mTOR.

PKI-587 *in vitro* profile in biomarker, caspase activation, and FOXO1-GFP translocation assays

***PKI-587 effect on phosphorylation of PI3K and mTOR effector proteins, and activation of caspase 3/7 in MDA-MB-361 [HER2$^+$, PIK3CA* (E545K)].** The effect of PKI-587 on a group of PI3K/mTOR effector proteins in MDA-MB-361 after 4 hours of exposure is shown in Fig. 2A. This linked PKI-587 enzyme inhibition to cellular antiproliferative effects. Suppression of cellular PIP3 by PKI-587 was indirectly shown by potent (IC_{50} < 3 nmol/L) suppression of phosphorylated Akt (p-Akt) at T308 (Fig. 2A). Full activation of Akt kinase occurs when the mTOR TORC2 protein complex phosphorylates Akt at S473. PKI-587 caused potent (IC_{50} < 10 nmol/L) suppression of p-Akt at S473 (Fig. 2A). Examples of PKI-587 mTOR TORC1 complex inhibition were suppression of 4EBP1 and p70S6 kinase (70S6K) phosphorylation at IC_{50} values of less than 3 nmol/L (Fig. 2A).

PKI-587 suppression of p-Akt caused consequent effects on Akt effectors such as PRAS40 (proline-rich Akt substrate, 40 kDa), ENOS (endothelial nitric oxide synthase), and GSK3 (glycogen synthase kinase 3). Akt phosphorylation of

Published OnlineFirst February 15, 2011; DOI: 10.1158/1078-0432.CCR-10-1694

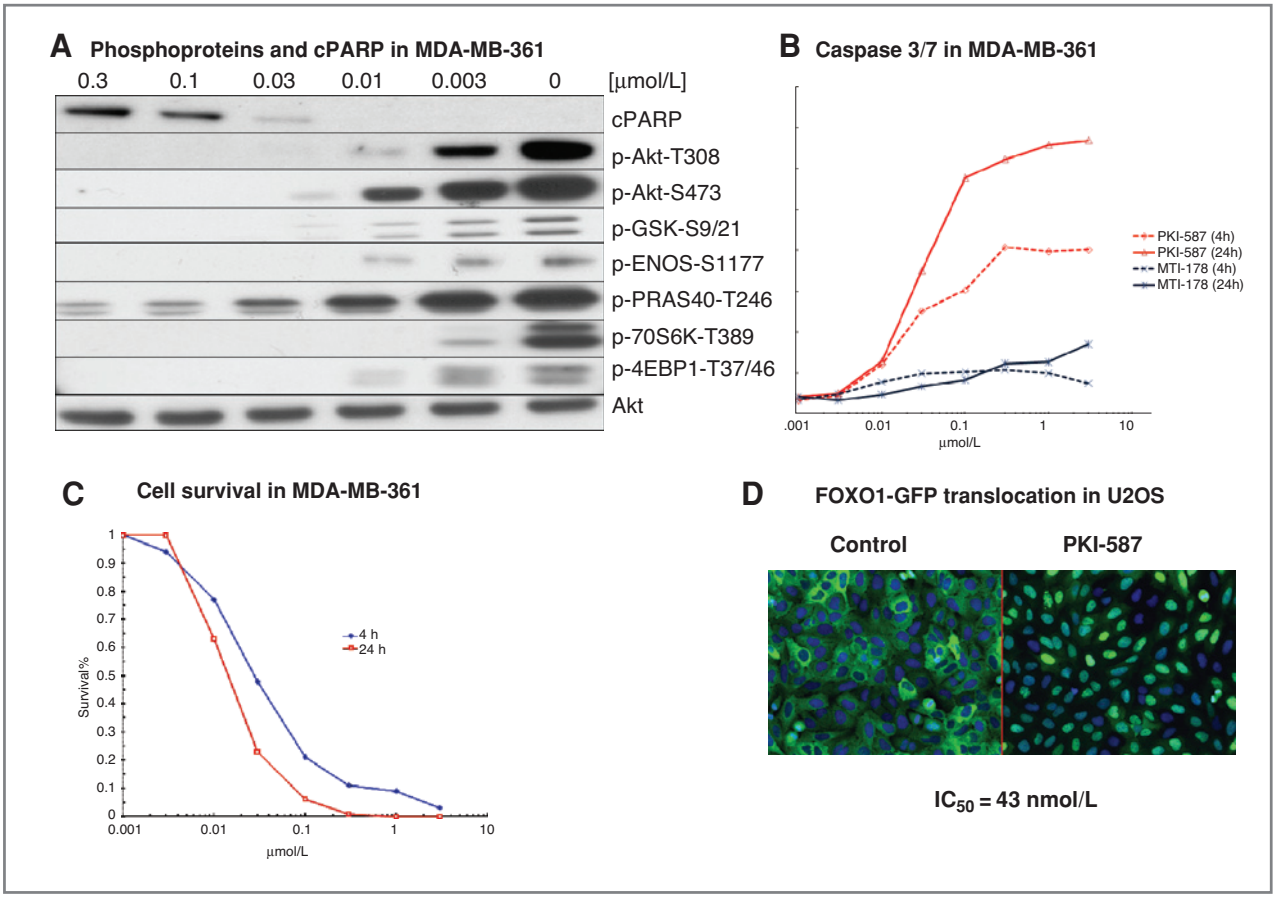

Figure 2. *In vitro* profile of PKI-587. MDA-MB-361 [HER2$^+$/*PIK3CA* (E545K)] cells were exposed to PKI-587 (0.003–0.3 μmol/L) for 4 hours. A, PKI-587 suppression of: p-Akt (T308 and S473); phosphorylation of Akt effectors [GSK3 (S9/21), PRAS40 (T246), and ENOS (S1177)]; phosphorylation of mTOR effectors [p70S6K (T389), p-4EBP1 (T37/46)]; and PKI-587 induction of cPARP at 0.03 μmol/L. B, caspase 3/7 activity in MDA-MB-361 after 4 and 24 hours of exposure to PKI-587 4 h = ◆, PKI-587 24 h = Δ or MTI-178 (selective mTOR inhibitor, MTI-178 4 h = X; MTI-178 24 h = ★). PKI-587 concentration (μmol/L) on the *x*-axis, luminescence units (LU) on the *y*-axis. C, MDA-MB-361 cell survival after 4 or 24 hours PKI-587 exposure, followed by compound removal and subsequent 24 hours incubation in complete growth media. Cell number was determined using a Cellomics Array Scan HCS reader. PKI-587 4 hours (◆), PKI-587 24 hours (□); concentration (μmol/L) on *x*-axis, survival % (1 = 100%) on *y*-axis. D, top, translocation of FOXO1-GFP (green) in U2OS from cytoplasm (left) to the nucleus (right) after 60 minutes of exposure to PKI-587 (IC_{50} = 43 nmol/L). Nuclei (blue) stained with Hoechst 33342.

PRAS40 at T246 was suppressed at an IC_{50} < 10 nmol/L (Fig. 2A). Akt phosphorylation of ENOS at S1177 and GSK-3α/GSK-3β at S9/S21 was suppressed by PKI-587 at IC_{50} values of less than 3 nmol/L (Fig. 2A).

In MDA-MB-361 cells, the effect of PKI-587 on the induction of cPARP, an indicator of cell apoptosis (23), was evident. Complete PKI-587 suppression of p-Akt in MDA-MB-361 correlated with detectable cPARP at 30 nmol/L PKI-587 (Fig. 2A). Cleaved PARP was detected in MDA-MB-361 within 1 hour after exposure to PKI-587 (Supplementary Fig. S2). PKI-587 did not affect the overall Akt level in MDA-MB-361 cells at concentrations tested (Fig. 2A).

Because caspase 3 is a critical mediator of apoptosis, associated with proteolytic cleavage of many key proteins, including the nuclear enzyme PARP (24, 25), we examined PKI-587 effect on this enzyme in MDA-MB-361. Figure 2B shows that PKI-587 caused a dose-dependent increase in caspase 3/7 activity at 4 and 24 hours. The increased caspase 3/7 activity caused by PKI-587 exceeded that caused by a highly selective mTOR kinase inhibitor, MTI-178 (26). In addition, only 6% of MDA-MB-361 cells exposed to 100 nmol/L PKI-587 for 24 hours remained viable (Fig. 2C).

PKI-587 effect on FOXO1(FKHR)-GFP translocation in U2OS. FOXO1 activity is regulated by Akt-mediated phosphorylation (27). Akt-phosphorylated FOXO1 is sequestered in the cytosol by 14–3-3 protein, and unphosphorylated FOXO1 locates to the cell nucleus. Figure 2D showed that PKI-587 suppression of p-Akt caused FOXO1-GFP translocation to cell nuclei in U2OS cells (Thermo Scientific). The IC_{50} value was 43 nmol/L for PKI-587 effect on FOXO1-GFP (Fig. 2D).

In vivo biomarker profile and efficacy of PKI-587 in MDA-MB-361 (breast) tumor xenografts

Initially, the biomarker targets p-Akt and cPARP were used to assess PKI-587 activity *in vivo*. Figure 3A shows that PKI-587 at 2 mg/kg (single dose) suppressed p-Akt

Published OnlineFirst February 15, 2011; DOI: 10.1158/1078-0432.CCR-10-1694

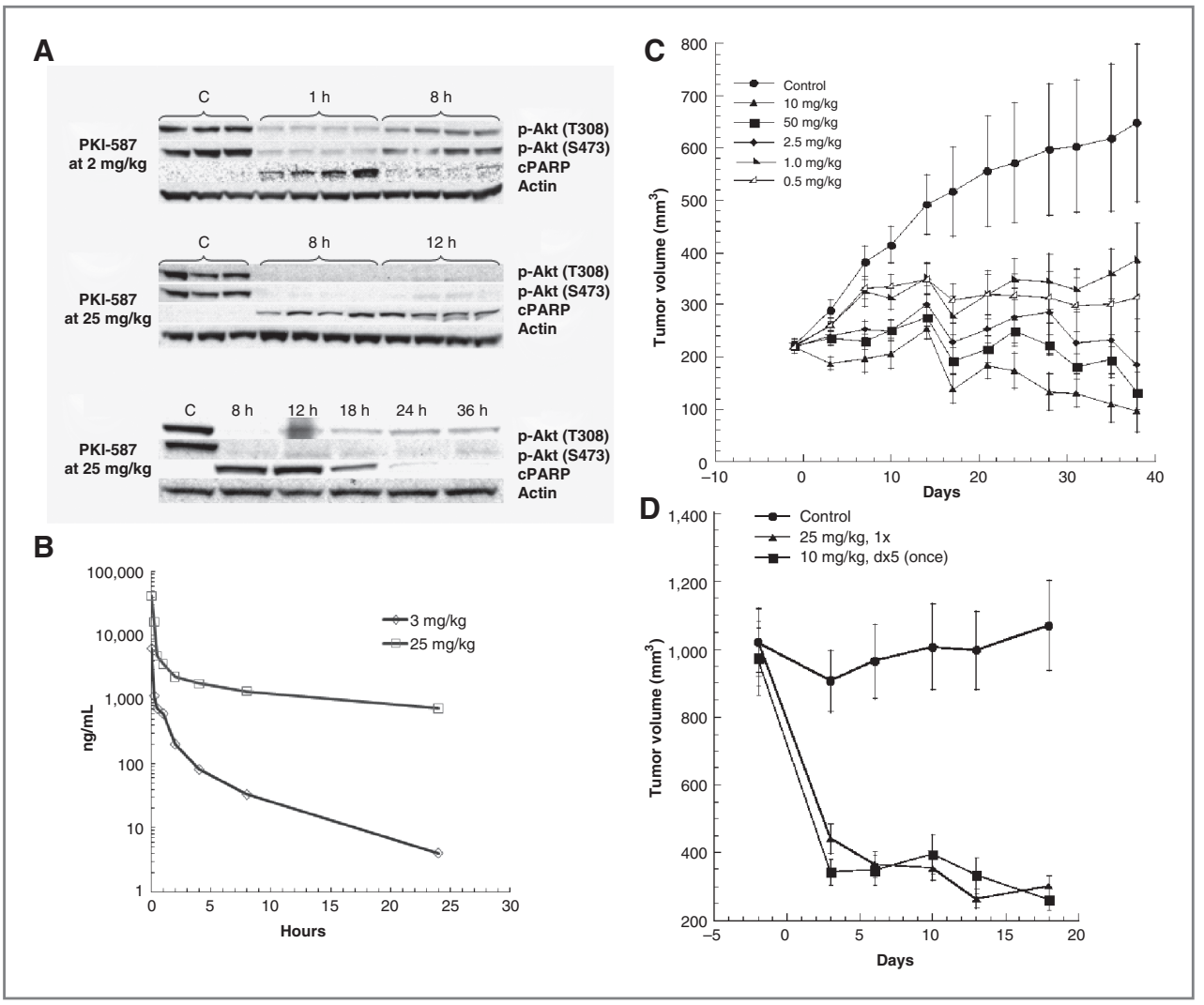

Figure 3. PKI-587 efficacy against MDA-MB361 xenografts. A, suppression of p-Akt (T308 and S473) and induction of cPARP in MDA-MB-361 tumor tissue from nude mice after single-dose exposure to 2 (top) or 25 (middle and bottom) mg/kg PKI-587. B, pharmacokinetic data from MDA-MB-361 tumor-bearing nude mice given PKI-587 at 3 and 25 mg/kg (single dose). C, PKI-587 dose response (0.5–10 mg/kg; d×5, 3 rounds, 2-day intervals between rounds). D, PKI-587 induced regression of large (~1,000 mm^3) MDA-MB-361 tumors. Regimen: 25 mg/kg once weekly or 10 mg/kg dx5 (1 round). For all *in vivo* studies, each data point represents the mean ± SEM tumor volume from 10 mice.

(T308 and S473) and induced cPARP at 1 hour in MDA-MB-361 tumor tissue grown in nude mice. At 8 hours, the effect on p-Akt diminished and cPARP was no longer evident. PKI-587 at 25 mg/kg (single dose) suppressed p-Akt (T308 and S473) for up to 36 hours, with cPARP still evident at 18 hours. Figure 3B shows phamacokinetic data for PKI-587 given to nude mice at 3 or 25 mg/kg (single dose). PKI-587 plasma half-life values at 3 and 25 mg/kg were 4.9 and 14.4 hours, respectively. Supplementary Table S5 shows a pharmacokinetic /safety summary for PKI-587.

Dose response for PKI-587 (0.5–10 mg/kg) in the MDA-MB-361 model for 5 days (d×5, 3 rounds, 2-day intervals between rounds) showed regression caused by PKI-587 at 5 and 10 mg/kg (Fig. 3C). PKI-587 shrank large (~1,000 mm^3) MDA-MB-361 tumors (Fig. 3D) when given at 25 mg/kg once weekly or at 10 mg/kg once daily for 5 days (d×5, 1 round). With an intermittent dosing schedule (days 1, 5, 9), minimal effective dose (≥50% tumor growth inhibition) was 3 mg/kg against MDA-MB-361 tumors (Supplementary Fig. S3A). PKI-587 at 20 mg/kg (day 1, 5, 9 regimen) had greater efficacy against MDA-MB-361 than taxol at 60 mg/kg (i.p., once; Supplementary Fig. S3B).

PKI-587 also had significant efficacy in the BT474 [breast; $HER2^+$, *PIK3CA* (K111N)] xenograft model when given at 5 and 10 mg/kg (day 1, 5, 9 regimen; Supplementary Fig. S4A and B). PKI-587 was well tolerated at all dosing levels described here and later. Single maximum tolerated dose (MTD) that affected animal viability was 30 mg/kg.

Published OnlineFirst February 15, 2011; DOI: 10.1158/1078-0432.CCR-10-1694

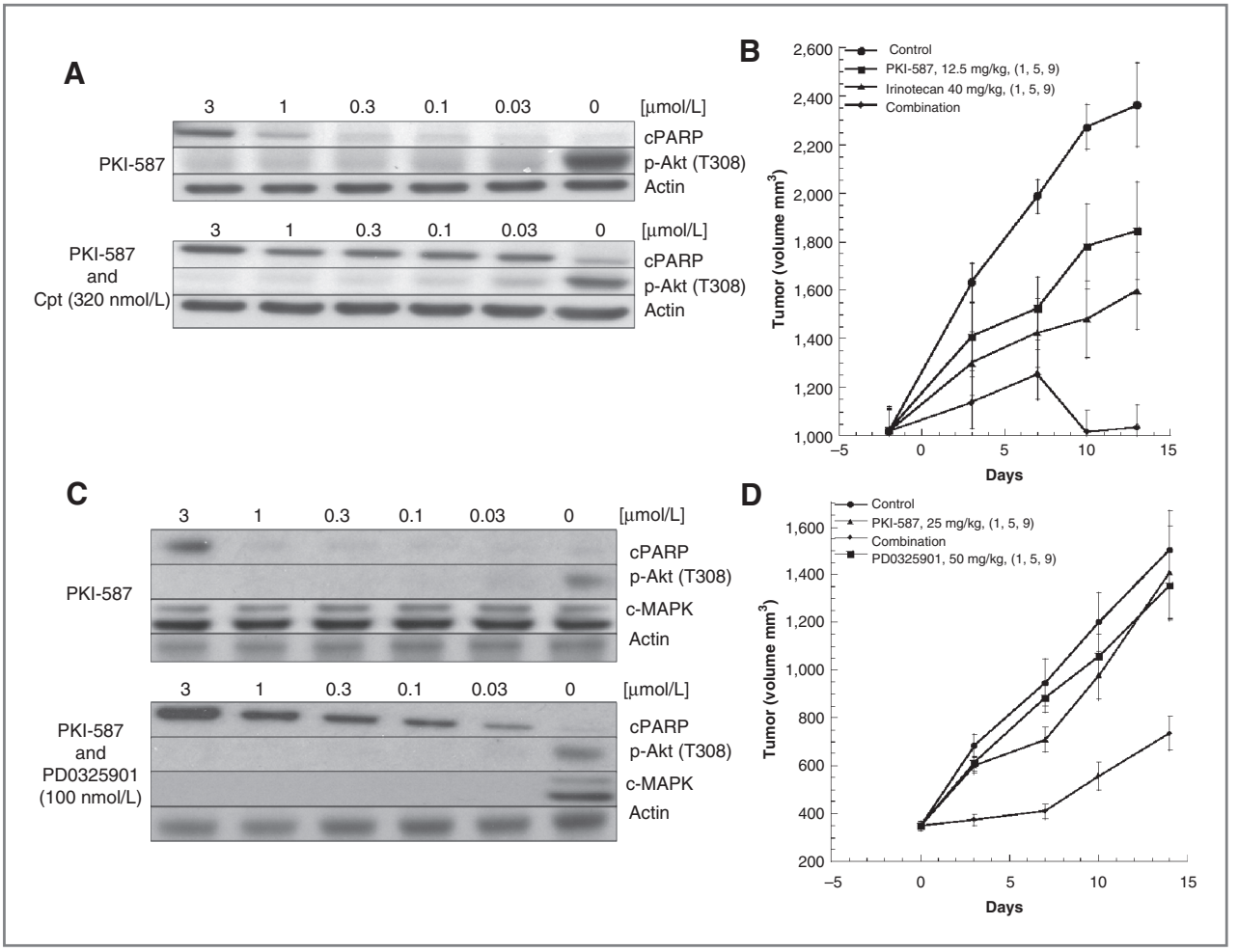

Figure 4. PKI-587 *in vitro* and *in vivo* efficacy against HCT116 colon tumor cells. A (*in vitro*), top, PKI-587 (alone) effect on p-Akt (T308) and cPARP; bottom, PKI-587/camptothecin (320 nmol/L) combination effect on p-Akt (T308) and cPARP (all at 18 hours). B, enhanced PKI-587 *in vivo* efficacy against large HCT116 tumors when combined with irinotecan (◆). C, PKI-587 *in vitro*: suppression (top) of p-Akt (T308), effect on p-MAPK, and cPARP induction; bottom, combined PKI-587 and PD0325901 (100 nmol/L) effect on the same markers (all at 24 hours). D, *in vivo* response of HCT116 tumors to PKI-587 alone (▲), PD0325901 alone (■), and PKI-587 (25 mg/kg)/PD0325901 (50 mg/kg) combination (◆). All compounds were given on a day 1, 5, 9 intermittent dosing schedule.

In vivo efficacy of PKI-587 in HCT116 (colon) tumor xenografts

In vivo regimens to test PKI-587 efficacy in the HCT116 [*K-Ras*, *PIK3CA* (H1047R)] model were guided by *in vitro* data. *In vitro*, PKI-587 inhibited HCT116 growth ($IC_{50} = 8$ nmol/L) and suppressed p-Akt (T308) at 30 nmol/L or more after 18 hours of exposure (Fig. 4A), but induction of cPARP was only evident at 3 μmol/L. To enhance PKI-587 *in vitro* efficacy against HCT116, we combined it with the cancer chemotherapeutics taxol, cisplatin, and camptothecin. Only camptothecin (topoisomerase I inhibitor) enhanced PKI-587 efficacy against HCT116. This effect occurred at a camptothecin concentration (320 nmol/L) that did not affect caspase 3/7 activity or induce cPARP. This combination increased caspase 3/7 activity (Supplementary Fig. S5A) and lowered cPARP induction to 30 nmol/L PKI-587 (Fig. 4A).

Against large (~1,000 mm^3) HCT116 tumor xenografts irinotecan (a semisynthetic camptothecin analogue) at 40 mg/kg, or PKI-587 at 12.5 mg/kg (day 1, 5, 9 regimen for both), only attenuated HCT116 tumor growth (Fig. 4B). Combined, irinotecan (40 mg/kg) and PKI-587 (12.5 mg/kg), day 1, 5, 9 regimen, prevented HCT116 tumor size increase in a 13-day study (Fig. 4B).

Because HCT116 cells have both *PIK3CA* and *K-Ras* mutations, we tested PD0325901 [MEK1/2 inhibitor; ref. 28] ability to enhance the PKI-587 *in vitro* effect on cPARP induction. The IC_{50} value of PD0325901 for *in vitro* growth inhibition of HCT116 was 230 nmol/L, and IC_{50} for phosphorylated mitogen-ctivated protein kinase [(p-MAPK) T202/Y204] suppression was 50 nmol/L (24 hours). Only minimal cPARP was detected in HCT116 after 24 hours of exposure to 3.0 μmol/L PD0325901. When PKI-587 and PD0325901 (100 nmol/L) were combined, increased

Published OnlineFirst February 15, 2011; DOI: 10.1158/1078-0432.CCR-10-1694

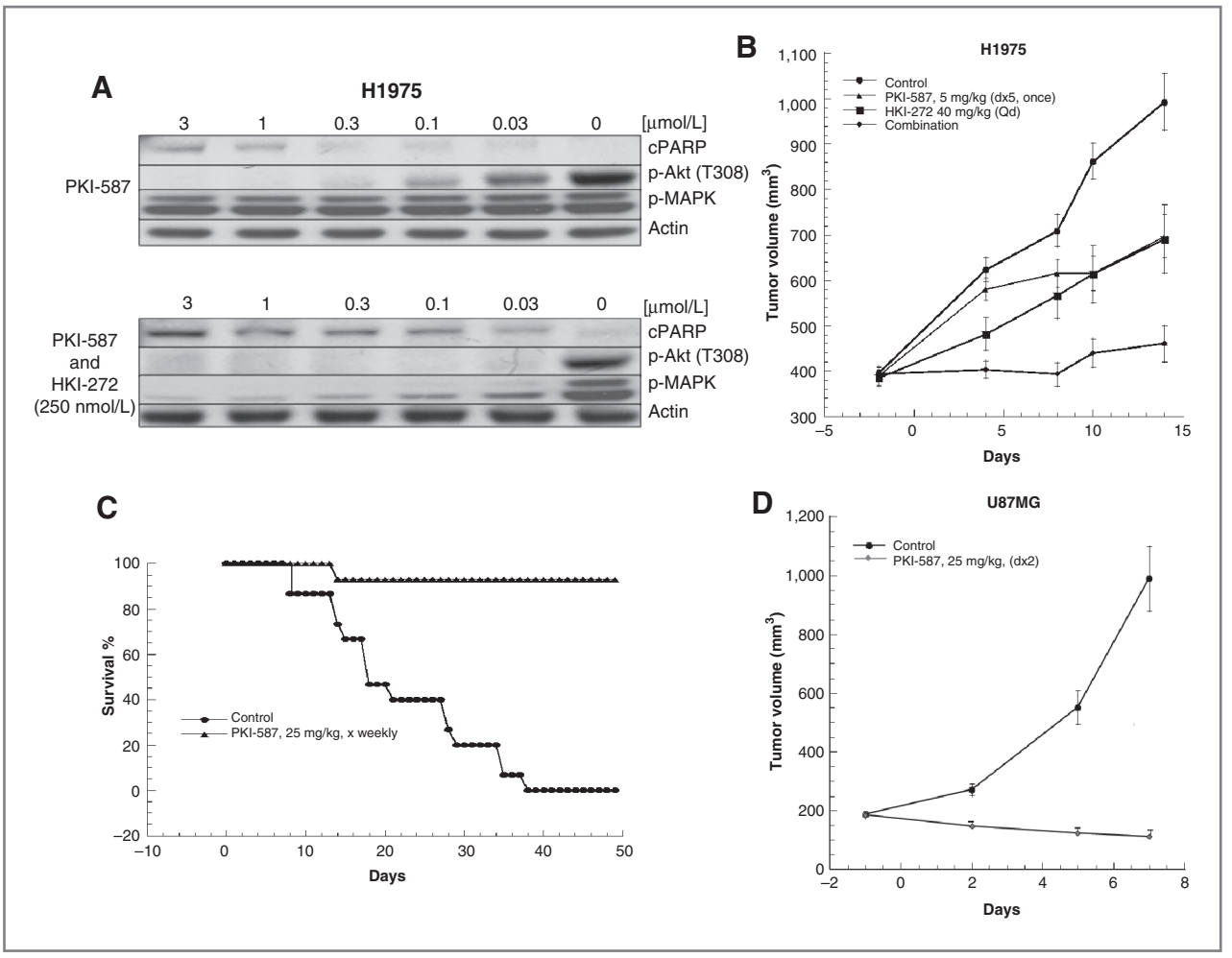

Figure 5. PKI-587 antitumor efficacy against H1975 (NSCLC), and U87MG (glioma) xenografts. A (*in vitro*), PKI-587 (alone) effect on p-Akt (T308), p-MAPK, and induction of cPARP (top); and PKI-587/HKI-272 (250 nmol/L) combination (bottom) effect on the same markers. B, enhanced antitumor effect of PKI-587 (5 mg/kg, dx5) combined with HKI-272 (40 mg/kg, every 14 days; ◆) compared with either compound alone. C, PKI-587 (25 mg/kg, once weekly; ▲) efficacy in an orthotopic version of the H1975 tumor model. Mouse death at day 8 in treatment group was not compound related. D, PKI-587 (at 25 mg/kg daily for 2 days) efficacy (regression) in the U87MG (*PTEN* negative) xenograft model.

caspase 3/7 activity was detected (Supplementary Fig. S5B) and cPARP was induced at 30 nmol/L or more PKI-587 (Fig. 4C).

Against small HCT116 tumor xenografts (~300 mm^3) either PKI-587 (25 mg/kg) or PD0325901 (50 mg/kg) alone (day 1, 5, 9 regimen) were ineffective (Fig. 4D). In combination, statistically significant ($P < 0.01$) antitumor efficacy was observed (Fig. 4D).

PKI-587 antitumor efficacy against H1975 (NSCLC) and U87MG (glioma) tumor xenografts

Efficacy of PKI-587 in H1975 (NSCLC) tumor xenografts. In a mouse transgenic lung tumor model driven by mutant, activated epidermal growth factor receptor [(EGFR); L858R and T790M], the combined antitumor effect of the irreversible HER2(neu)/EGFR inhibitor HKI-272 and the mTOR inhibitor rapamycin was greater than that observed for either compound alone (29). HKI-272 overcomes resistance the L858R/T790M EGFR mutant displays against reversible inhibitors such as Iressa and Tarceva (30). We therefore tested the efficacy of PKI-587 alone, or with HKI-272, in a human NSCLC tumor line equivalent to the mouse lung tumor model. We used H1975 that has L858R and T790M mutant EGFR (30).

In vitro, PKI-587 inhibited H1975 growth (IC_{50} = 14 nmol/L), suppressed p-Akt (T308; IC_{50} = 30 nmol/L), induced caspase 3/7 activity at 300 nmol/L or more (Supplementary Fig. S5C), caused cPARP induction at 1 μmol/L (Fig. 5A), and did not affect p-MAPK (Supplementary Fig. S9B). HKI-272 alone also suppressed p-Akt (T308; IC_{50} = 350 nmol/L), suppressed p-MAPK (IC_{50} = 250 nmol/L; Supplementary Fig. S9A), and induced caspase 3/7 and cPARP at 3 μmol/L. Exposure (24 hours) of H1975 to combined PKI-587 and HKI-272 (250 nmol/L)

Published OnlineFirst February 15, 2011; DOI: 10.1158/1078-0432.CCR-10-1694

markedly increased suppression of p-Akt (T308; IC_{50} < 30 nmol/L), increased caspase 3/7 activity (Supplementary Fig. 5C), and induced cPARP at 30 nmol/L or more (Fig. 5A).

These data suggested that *in vivo* combined PKI-587 and HKI-272 could be more effective than either compound alone. When PKI-587 (5 mg/kg, d×5 once) was given in combination with HKI-272 (40 mg/kg, po daily) significantly ($P < 0.02$), more antitumor effect than either compound given alone was observed in a 14-day study (Fig. 5B). In the combination group, tumors were 35% smaller at day 14 than with PKI-587 or HKI-272 alone, and tumor size in the combination group was 54% smaller than untreated controls. In addition, at all measurement times, combination treatment outperformed either compound given alone.

PKI-587 also showed single-agent efficacy in the H1975 model, including tumor regression at early time points after continuous dosing at more than 5 mg/kg (Supplementary Fig. S6). Furthermore, PKI-587 showed antitumor activity in an orthotopic version of the H1975 xenograft model. Nude mice with H1975 cells injected into their pleural cavity were given 25 mg/kg PKI-587 weekly. Only 1 mouse in the treatment group (10 mice per group) died, but the death was not tumor or compound related (Fig. 5C). In contrast, at day 40, all untreated animals were dead. PKI-587 at 20 mg/kg in an intermittent (day 1, 5, 9) regimen was equally effective in the H1975 orthotopic lung cancer model (Supplementary Fig. S7).

Efficacy of PKI-587 in U87MG (glioma) tumor xenografts. PKI-587 efficacy was tested in the U87MG glioblastoma multiforme [(GBM) *PTEN* negative] xenograft model, which has rapid, aggressive growth. At 25 mg/kg, daily for 2 days (d×2), PKI-587 caused U87MG tumor regression (Fig. 5D). PKI-587 at 25 mg/kg (d×2) caused mice to become pale and lethargic, but all animals recovered subsequent to compound cessation. PKI-587 tested at 1.56 to 12.5 mg/kg (d×5, dose–response regimen) caused significant ($P < 0.01$) tumor growth inhibition at all dosing levels. PKI-587 at 12.5 and 6.25 mg/kg resulted in 78% and 86% reduction in tumor growth, respectively, at day 10 compared with control group (Supplementary Fig. S8). PKI-587 at both 6.25 and 12.5 mg/kg had a cytostatic effect on U87MG tumors.

Discussion

PKI-587 was the most potent Wyeth PI3K/mTOR inhibitor advanced to clinical development. Its preclinical profile places it among the most potent dual PI3K/mTOR inhibitors reported to date (7, 8). It had subnanomolar IC_{50} values against wild-type and mutant forms of PI3K-α, and IC_{50} values of less than 100 nmol/L in 50 of 59 tumor cell lines tested (Table 1, Supplementary Table S1). *In vitro*, PKI-587 suppression of p-Akt closely correlated with tumor cell growth suppression. PKI-587 potency translated into a broad range of *in vivo* efficacy in MDA-MB-361, BT474, H1975, U87MG, and HCT116 tumor models. These models have reported genetic changes that aberrantly upregulate PI3K signaling including *PIK3CA* mutation (E545K, H1047R, K111N), receptor tyrosine kinase (RTK) overexpression ($HER2^+$), *RTK* mutation (EGFR; L858R, T790M), *PTEN* phosphatase inactivation, or *K-Ras* mutation (2, 5–8, 18). PKI-587 caused regression in MDA-MB-361 [$HER2^+$/*PIK3CA* (E545K)], H1975 (EGFR, L858R/T790M), and U87MG (*PTEN*) models. MDA-MB-361 was the most sensitive to PKI-587, whereas HCT116 [*K-Ras*, *PIK3CA* (H1047R)] was less responsive. The PKI-587 antitumor efficacy gradient was as follows: MDA-MB-361, BT474 > H1975, U87MG > HCT116.

In MDA-MB-361 cells, PKI-587 activated caspase 3/7, induced cPARP, and caused cell death after relatively short exposure times (Fig. 2A–C; Supplementary Fig. S2A). Furthermore, PKI-587 caused much more rapid and extensive activation of caspase 3/7 and cPARP induction in MDA-MB-361 than the highly selective mTOR inhibitor MTI-178 (Fig. 2C; Supplementary Fig. S2B). The effects of PKI-587 or MTI-178 on caspase 3/7 activation and induction of cPARP coincided with PKI-587 suppression of p-Akt at T308 and not p-Akt at S473 (Supplementary Fig. S2B). This strongly indicates that some PKI-587–sensitive components of the PI3K/Akt portion of the PI3K/Akt/mTOR signaling pathway regulate MDA-MB-361 cell survival. More sophisticated analysis (e.g., phosphoproteomics, expression profiling) may reveal what factor(s) is responsible for acute MDA-MB-361 sensitivity to PKI-587 and possibly point to novel drug discovery target(s).

In the MDA-MB-361 xenograft model, PKI-587 suppressed Akt phosphorylation (T308 and S473), induced cPARP, and when given at sufficient levels, caused tumor regression (Fig. 3D; Supplementary Fig. S3B). PKI-587 at 2 mg/kg suppressed p-Akt and induced cPARP at 1-hour postadministration, but this effect dissipated at 8 hours (Fig. 3A). PKI-587 at equivalent doses (1–3.125 mg/mL, Fig. 3A; Supplementary Fig. S3) only attenuated tumor growth. PKI-587 at 25 mg/kg (single dose) suppressed p-Akt (T308 and S473) for up to 36 hours and cPARP was evident for up to 18 hours (Fig. 3A). PKI-587 at 25 mg/kg (once weekly) rapidly shrank large MDA-MB-361 tumors (tumor volume of ∼1,000 mm^3 reduced to ∼230 mm^3; Fig. 3D) and suppressed tumor re-growth. Data from the MDA-MB-361 model indicate that tumor regression correlated with durable p-Akt suppression, a result of the potency and long plasma half-life of PKI-587.

Not surprisingly, the HCT116 colon model with mutant *K-Ras* and PI3K-α, was refractory to PKI-587. This was consistent with data from various studies evaluating PI3K inhibitor efficacy in tumor models with mutant *K-Ras*. Combining PKI-587 with a MEK inhibitor in the HCT116 model was an obvious choice because such combinations mitigate resistance to PI3K inhibitors found in tumor cell lines harboring mutant *K-Ras* (31–34). *In vitro* the proapoptotic effects of PKI-587 were greatly enhanced when it was combined with PD0325901 (Fig. 4C), and

in vivo the antitumor effect of combined PKI-587 and PD0325901 exceeded that achieved by either compound alone. Positive outcome from this combination study in HCT116 suggests that PKI-587 along with Ras/MAPK signaling inhibitors may achieve clinical response in cancers driven by mutant *K-Ras*.

We also tested PKI-587 in combination with cisplatin, taxol, and camptothecin in the HCT116 model. We chose these agents because they are standard-of-care colon cancer treatments (35). Only the camptothecin/PKI-587 (*in vitro*) or irinotecan (camptothecin analogue)/PKI-587 (*in vivo*) combinations showed enhanced efficacy. In cells, camptothecin causes covalent topoisomerase I–DNA complexes (36), which reportedly convert into DNA double-strand breaks on collision with the replication fork (36). This induces p53-mediated DNA damage response and cell-cycle arrest at G_2/M (36, 37). In HCT116, Akt activation may allow these cells to bypass DNA damage–associated G_2 arrest (36, 37). Inhibition of Akt activation by PKI-587 may account for enhanced *in vivo* antitumor effects of the PKI-587/irinotecan combination against HCT116. Data in Figure 4B suggests that our hypothesis may be correct, but only further experimental data will confirm this.

PKI-587 showed single-agent efficacy in both xenograft and orthotopic versions of the H1975 [NSCLC; EGFR (L858R/T790M)] model. In H1975 xenografts, continuous dosing of PKI-587 (at >5 mg/kg) caused early time point tumor regression. In the H1975 orthotopic model, 25 mg/kg PKI-587 (weekly) kept (9 of 10) treated mice alive, whereas all control mice (10 of 10) were dead by day 40. This suggests that PKI-587 could be used against lung tumors that have acquired resistance to EGFR inhibitors such as Iressa or Tarceva. PKI-587 may also be effective in lung tumors that have acquired resistance to HER2/EGFR inhibitors by MET amplification or IGF-IR (insulin-like growth factor I receptor) or AXL activation (38, 39). PKI-587 efficacy in tumors driven by these RTKs will hinge on their dependence on PI3K/mTOR signaling for growth and survival. Because these RTKs activate both PI3K/mTOR and Ras/MAPK signaling pathways, PKI-587 in combination with targeted agents that inhibit Ras/MAPK signaling (e.g., PD0325901, HKI-272, herceptin) should be tested. Indeed, the antitumor efficacy of concomitant inhibition of the PI3K/mTOR and Ras/MAPK signaling pathways has been shown in NSCLC, breast, and colon tumor models (31–34, 40, 41). In H1975, HKI-272 suppression of p-MAPK (Fig. 5A) enhanced PKI-587 *in vitro* efficacy. This combination improved PKI-587–mediated caspase 3/7 activation and cPARP induction *in vitro* and, more importantly, improved PKI-587 antitumor efficacy *in vivo* (Supplementary Fig. S5C; Fig. 5A and B). Clinical outcome for NSCLC is especially bleak (42), and further investigation of PKI-587 alone and in combination with Ras/MAPK signaling inhibitors in NSCLC models should help direct PKI-587 clinical development.

In the aggressive glioma model, U87MG (*PTEN* negative), 25 mg/kg PKI-587 for 2 consecutive days caused tumor regression. However, this occurred near the limit of tolerated exposure in nude mice. Lower dosing regimens (1.56–12.5 mg/kg, d×5) were well tolerated and effectively suppressed U87MG tumor growth (Supplementary Fig. S8). Patients with *PTEN*-negative GBM tumors in general have a poor prognosis (43). In clinical settings, gliomas are resistant to EGFR inhibitors, radiotherapy, and most alkylating agents (44). In GBM, PKI-587 may be efficacious either as a single agent or in combination with cytostatic or cytotoxic drugs. Good rationale for testing such combinations derives from data showing that the Novartis PI3K/mTOR inhibitor BEZ235 combined with temozolomide caused U87MG tumor xenograft regression (7).

A key question about PI3K/mTOR signaling inhibitors has been: Can they cause tumor regression in preclinical models? Some compounds (e.g., PKI-402, GDC-0941) have positively answered this question (23, 45). But here we show how the very potent PKI-587 profile caused regression (e.g., U87MG model) at lower and/or less frequent dosing regimens than those reported for other PI3K pathway signaling inhibitors. An example of this is the comparison of PKI-587 with PKI-402, a PI3K/mTOR inhibitor we previously reported (23). In the aggressive U87MG glioma tumor model, used as a critical potency test, PKI-402 at 100 mg/kg (d×5, near MTD) only attenuated U87MG xenograft tumor growth (23). PKI-587 at just 25 mg/kg (d×2) caused U87MG tumor regression (Fig. 5D). Less efficacy by PKI-402 in the U87MG model correlated with a shorter 3.5 hour plasma half-life than that of the 14.4 hours for PKI-587 (25 mg/kg single dose, both). The compelling efficacy profile of PKI-587 will be more firmly established by direct experimental comparison of PKI-587 with other PI3K/mTOR signaling inhibitors.

Finally, unlike cytostatic PI3K inhibitors that cause tumor cell G_0/G_1 arrest (45–47), potent PKI-587 inhibition of class 1 PI3Ks can fully inhibit Akt activation and cause apoptosis induction (e.g., MDA-MB-361 model). This is the desired outcome against cancer cells. PKI-587 antitumor efficacy and its favorable drug safety profile in toxicology studies enabled it to enter phase 1 clinical evaluation in December 2009.

Disclosure of Potential Conflicts of Interest

No potential conflicts of interest were disclosed.

Acknowledgments

We thank Ker Yu and Lourdes Toral-Barza for evaluating PKI-587 in mTOR kinase and cellular assays and Veronica Soloveva for FOX1-GFP assay work.

The costs of publication of this article were defrayed in part by the payment of page charges. This article must therefore be hereby marked *advertisement* in accordance with 18 U.S.C. Section 1734 solely to indicate this fact.

Received June 29, 2010; revised February 4, 2011; accepted February 7, 2011; published OnlineFirst February 15, 2011.

Published OnlineFirst February 15, 2011; DOI: 10.1158/1078-0432.CCR-10-1694

References

1. Engelman JA, Luo J, Cantley LC. The evolution of phosphatidylinositol 3-kinases as regulators of growth and metabolism. Nat Rev Genet 2006;7:606–19.
2. Shaw RJ, Cantley LC. Ras, PI(3)K and mTOR signaling controls tumor cell growth. Nature 2006;441:424–30.
3. Kok K, Geering B, Vanhaesebroeck B. Regulation of phosphoinositide 3-kinase expression in health and disease. Trends Biochem Sci 2009;34;115–27.
4. Vanhaesebroeck B, Leevers SJ, Ahmadi K, Timms J, Katso R, Driscoll PC, et al. Synthesis and function of 3-phosphorylated inositol lipids. Annu Rev Biochem 2001;70:535–602.
5. Yuan TL, Cantley LC. PI3K pathway alterations in cancer: variations on a theme. Oncogene 2008;27:5497–510.
6. Keniry M, Parsons R. The role of PTEN signaling perturbations in cancer and in targeted therapy.Oncogene 2008;27:5477–85.
7. Maira SM, Stauffer F, Brueggen J, Furet P, Schnell C, Fritsch C, et al. Identification and characterization of NVP-BEZ235, a new orally available dual phosphatidylinositol 3-kinase/mammalian target of rapamycin inhibitor with potent in vivo antitumor activity. Mol Cancer Ther 2008;7:1851–63.
8. Engelman JA. Targeting PI3K signaling in cancer: opportunities, challenges, and limitations. Nat Rev Cancer 2009;9:550–62.
9. Liu P, Cheng H, Roberts TM, Zhao JJ. Targeting the phosphoinositide 3–kinase pathway in cancer. Nat Rev Drug Discov 2009;8:627–44.
10. Garlich JR, De P, Dey N, Su JD, Peng X, Miller A, et al. A vascular targeted pan phosphoinositide 3-kinase inhibitor prodrug, SF1126, with antitumor and antiangiogenic activity. Cancer Res 2008;68:206–15.
11. Dehnhardt CM, Venkatesan AM, Delos Santos E, Chen Z, Santos O, Ayral-Kaloustian S, et al. Lead optimization of *N*-3-substituted 7-morpholinotriazolopyrimidines as dual phosphoinositide 3-kinase/mammalian target of rapamycin inhibitors: discovery of PKI-402. J Med Chem 2009;53:798–810.
12. Folkes AJ, Ahmadi K, Alderton WK, Alix S, Baker SJ, Box G, et al. The identification of 2-(1*H*-indazol-4-yl)-6-(4-methanesulfonyl-piperazin-1-ylmethyl)-4-morpholin-4-yl-thieno[3,2-*d*]pyrimidine (GDC-0941) as a potent, selective, orally bioavailable inhibitor of class I PI3 kinase for the treatment of cancer. J Med Chem 2008;51:5522–32.
13. Herman SE, Gordon AL, Wagner AJ, Heerema NA, Zhao W, Flynn JM, et al. The phosphatidylinositol 3-kinase-δ inhibitor CAL-101 demonstrates promising pre-clinical activity in chronic lymphocytic leukemia by antagonizing intrinsic and extrinsic cellular survival signals. Blood 2010 Jun 3. [Epub ahead of print].
14. Chow S, Chew W, Berggren MI, et al. . Molecular pharmacology and antitumor activity of PX-866, a novel inhibitor of phosphoinositide-3-kinase signaling. Mol Cancer Ther 2004;3:763–72.
15. Venkatesan AM, Dehnhardt CM, Delos Santos E, Chen Z, Dos Santos O, Ayral-Kaloustian S, et al. Bis-Morpholino-1,3,5-triazine derivatives: potent, ATP-competitive phosphatidylinositol-3-kinase (PI3K)/mammalian target of rapamycin (mTOR) inhibitors: discovery of PKI-587 a highly efficacious dual inhibitor. J Med Chem 2010;53:2636–45.
16. Yang X, Li P, Feldberg L, Kim SC, Bowman M, Hollander I, et al. A directly labeled TR-FRET assay for monitoring phosphoinositide-3-kinase activity. Comb Chem High Throughput Screen 2006;9:565–70.
17. Mallon R, Hollander I, Feldberg L, Lucas J, Soloveva V, Venkatesan A, et al. Anti-tumor efficacy profile of PKI-402, a dual PI3K/mTOR inhibitor. Mol Cancer Ther 2010;9:976–84.
18. Wellcome Trust Sanger Institute. Available from: http://www.sanger.ac.uk/genetics/CGP/cosmic.
19. Carson JD, Van Aller G, Lehr R, Sinnamon RH, Kirkpatrick RB, Auger KR, et al. Effects of oncogenic p110alpha subunit mutations on the lipid kinase activity of phosphoinositide 3-kinase. Biochem J 2008;409:519–24.
20. Grossi A, Biscardi M. Reversal of MDR by verapamil analogues. Hematology 2004;9:47–56.
21. Chiu LY, Ko JL, Lee YJ, Yang TY, Tee YT, Sheu GT. L-type calcium channel blockers reverse docetaxel and vincristine-induced multidrug resistance independent of ABCB1 expression in human lung cancer cell lines. Toxicol Lett 2010;15:408–18.
22. Toffoli G, Viel A, Tumiotto L, Biscontin G, Rossi C, Boiocchi M. Pleiotropic-resistant phenotype is a multifactorial phenomenon in human colon carcinoma cell lines. Br J Cancer 1991;63:51–6.
23. Oliver FJ, de la Rubia G, Rolli V, Ruiz-Ruiz MC, de Murcia G, Murcia JM. Importance of poly(ADP-ribose) polymerase and its cleavage in apoptosis. Lesson from an uncleavable mutant. J Biol Chem 1998;273:33533–9.
24. Tewari M, Quan LT, O'Rourke K, Desnoyers S, Zeng Z, Beidler DR, et al. Yama/CPP32 beta, a mammalian homolog of CED-3, is a CrmA-inhibitable protease that cleaves the death substrate poly(ADP-ribose) polymerase. Cell 1995;81:801–9.
25. Fernandes-Alnemri T, Litwack G, Alnemri ES. CPP32, a novel human apoptotic protein with homology to *Caenorhabditis elegans* cell death protein Ced-3 and mammalian interleukin-1 beta-converting enzyme. J Biol Chem 1994;269:30761–4.
26. Verheijen JC, Richard DJ, Curran K, Kaplan J, Lefever M, Nowak P, et al. Discovery of 4-Morpholino-6-aryl-1*H*-pyrazolo[3,4-*d*]pyrimidines as highly potent and selective ATP-competitive inhibitors of the mammalian target of rapamycin (mTOR): optimization of the 6-aryl substituent. J Med Chem 2009;52:8010–24.
27. Arden KC. FoxO: linking new signaling pathways. Mol Cell 2004;14:416–8.
28. Sebolt-Leopold JS. Advances in the development of cancer therapeutics directed against the RAS-mitogen-activated protein kinase pathway. Clin Cancer Res 2008;14:3651–6.
29. Li D, Shimamura T, Ji H, Chen L, Haringsma HJ, McNamara K, et al. Bronchial and peripheral murine lung carcinomas induced by T790M-L858R mutant EGFR respond to HKI-272 and rapamycin combination therapy. Cancer Cell 2007;12:81–93.
30. Kwak EL, Sordella R, Bell DW, Godin-Heymann N, Okimoto RA, Brannigan BW, et al. Irreversible inhibitors of the EGF receptor may circumvent acquired resistance to gefitinib. Proc Natl Acad Sci U S A 2005;102:7665–70.
31. Wee S, Jagani Z, Xiang KX, Loo A, Dorsch M, Yao YM, et al. PI3K pathway activation mediates resistance to MEK inhibitors in KRAS mutant cancers. Cancer Res 2009;69:4286–93.
32. Engelman JA, Chen L, Tan X, Crosby K, Guimaraes AR, Upadhyay R, et al. Effective use of PI3K and MEK inhibitors to treat mutant Kras G12D and PIK3CA H1047R murine lung cancers. Nat Med 2008;14:1351–6.
33. Sos ML, Fischer S, Ullrich R, Peifer M, Heuckmann JM, Koker M, et al. Identifying genotype-dependent efficacy of single and combined PI3K- and MAPK-pathway inhibition in cancer. Proc Natl Acad Sci U S A 2009;106:18351–6.
34. Konstantinidou G, Bey EA, Rabellino A, Schuster K, Maira MS, Gazdar AF, et al. Dual phosphoinositide 3-kinase/mammalian target of rapamycin blockade is an effective radiosensitizing strategy for the treatment of non-small cell lung cancer harboring K-RAS mutations. Cancer Res 2009;69:7644–52.
35. Yim KL, Cunningham D. Chemotherapy: optimizing irinotecan regimens for colorectal cancer. Nat Rev Clin Oncol 2009;6:560–1.
36. Liu LF, Desai SD, Li TK, Mao Y, Sun M, Sim SP. Mechanism of action of camptothecin. Ann N Y Acad Sci 2000;922:1–10.
37. Ashcroft M, Taya Y, Vousden KH. Stress signals utilize multiple pathways to stabilize p53. Mol Cell Biol 2000;20:3224–33.
38. Engelman JA, Zejnullahu K, Mitsudomi T, Song Y, Hyland C, Park JO, et al. MET amplification leads to gefitinib resistance in lung cancer by activating ERBB3 signaling. Science 2007;316:1039–43.
39. Liu L, Greger J, Shi H, Liu Y, Greshock J, Annan R, et al. Novel mechanism of lapatinib resistance in HER2-positive breast tumor cells: activation of AXL. Cancer Res 2009;69:6871–8.
40. Faber AC, Li D, Song Y, Liang MC, Yeap BY, Bronson RT, et al. Differential induction of apoptosis in HER2 and EGFR addicted cancers following PI3K inhibition. Proc Natl Acad Sci U S A 2009;106:19503–8.
41. Hoeflich KP, O'Brien C, Boyd Z, Cavet G, Guerrero S, Jung K, et al. *In vivo* antitumor activity of MEK and phosphatidylinositol 3-kinase

Published OnlineFirst February 15, 2011; DOI: 10.1158/1078-0432.CCR-10-1694

inhibitors in basal-like breast cancer models. Clin Cancer Res 2009;15:4649–64.
42. Sharma SV, Bell DW, Settleman J, Haber DA. Epidermal growth factor receptor mutations in lung cancer. Nat Rev Cancer 2007;7:169–81.
43. Mellinghoff IK, Wang MY, Vivanco I, Haas-Kogan DA, Zhu S, Dia EQ, et al. Molecular determinants of the response of glioblastomas to EGFR kinase inhibitors. N Engl J Med 2005;353:2012–24.
44. Norden AD, Drappatz J, Wen PY. Novel anti-angiogenic therapies for malignant gliomas. Lancet Neurol 2008;7:1152–60.
45. Raynaud FI, Eccles S, Clarke PA, Hayes A, Nutley B, Alix S, et al. Pharmacologic characterization of a potent inhibitor of class I phosphatidylinositide 3-kinases. Cancer Res 2007;67:5840–50.
46. Dan S, Yoshimi H, Okamura M, Mukai Y, Yamori T. Inhibition of PI3K by ZSTK474 suppressed tumor growth not via apoptosis but G0/G1 arrest. Biochem Biophys Res Commun 2009;379:104–9.
47. Fan QW, Cheng CK, Nicolaides TP, Hackett CS, Knight ZA, Shokat KM, et al. A dual phosphoinositide-3-kinase alpha/mTOR inhibitor cooperates with blockade of epidermal growth factor receptor in PTEN-mutant glioma. Cancer Res 2007;67:7960–5.

Published OnlineFirst February 15, 2011; DOI: 10.1158/1078-0432.CCR-10-1694

Clinical Cancer Research

Antitumor Efficacy of PKI-587, a Highly Potent Dual PI3K/mTOR Kinase Inhibitor

Robert Mallon, Larry R. Feldberg, Judy Lucas, et al.

Clin Cancer Res 2011;17:3193-3203. Published OnlineFirst February 15, 2011.